https://doi.org/10.5194/egusphere-2025-414
Preprint. Discussion started: 14 February 2025

How does the time shift between precipitation and evaporation affect annual streamflow variability? A large sample elasticity study

Vazken Andréassian[*,1], Guilherme Mendoza Guimarães[1], Alban de Lavenne[1], Julien Lerat[2]

[1] Université Paris-Saclay, INRAE, HYCAR Research Unit, Antony, France
[2] CSIRO, Canberra, Australia
[*]Corresponding author : Vazken Andréassian, vazken.andreassian@inrae.fr

Abstract

One of the most basic questions asked to hydrologists is that of the quantification of catchment response to climatic variations, i.e. that of the variations around the average annual flow given the climatic anomaly of a given year. This paper presents a large sample analysis based on 4122 catchments from four continents, where we investigate how annual streamflow variability depends on climate variables – rainfall and potential evaporation – and on the season when precipitation occurs, i.e. on the synchronicity between precipitation and potential evaporation. We use catchment data to verify the existence of this link, and show that, in all countries and under the main climates represented, synchronicity anomalies come as the second most important factor to explain annual streamflow anomalies: after precipitation but before potential evaporation. Introducing the synchronicity between precipitation and potential evaporation as an independent variable improves the prediction of annual streamflow variability significantly.

Keywords: annual streamflow anomalies, elasticity, sensitivity, seasonality

Notations

We deal in this paper with three hydrological fluxes: precipitation (P_n), streamflow (Q_n) and potential evaporation (E_{0n}). The three fluxes are computed at catchment scale,

https://doi.org/10.5194/egusphere-2025-414
Preprint. Discussion started: 14 February 2025

expressed in millimetres per year, and represent annual sums (index n refers to the year in question). We use a hydrological year from October 1st of year $n-1$ to September 30th of year n in the Northern hemisphere and from April 1st of year n to March 31st of year $n+1$ in the Southern hemisphere. Anomalies (of P, Q and E_0), noted Δ, are computed as the difference between the annual value and the long-term average value, i.e. $\Delta Q_n = Q_n - \bar{Q}$, $\Delta P_n = P_n - \bar{P}$, etc.

1 Introduction

1.1 On the climate elasticity of streamflow

To assess the impact of climate change on water resources, hydrologists need to quantify the response of catchment flow with respect to variations in climatic conditions. For this, they estimate the climate elasticity of streamflow (Schaake and Liu, 1989). The hydrologic literature and hydrologic common sense both suggest that the best predictor of the annual streamflow anomaly is the annual precipitation anomaly (e.g. Pardé, 1933a; Leopold, 1974). In addition, many elasticity studies have also considered the anomaly of potential evaporation, although it is usually only weakly significant in regression studies. In this paper, we focus on a third explanatory variable quantifying the synchronicity between precipitation and potential evaporation within the year.

1.2 Linear models to predict streamflow anomalies

There is an abundant literature concerning elasticity studies in hydrology, and our work comes in the continuation of the earlier empirical (i.e. measurement-based) studies of Sankarasubramanian et al. (2001), Chiew (2006) and Andréassian et al. (2016). Here, we follow the same principle and use linear regression models based on measured annual data to evaluate the climate elasticity of streamflow. An alternative approach to estimate climate elasticities would consist in using hydrological models of various complexities (e.g. Koster and Suarez, 1999). However, even if models are powerful investigative tools, they also rely on restrictive assumptions that often limit their credibility outside of a calibration range. This can be particularly problematic in a large-scale study on the impact of climate change. Thus, we favoured an approach

https://doi.org/10.5194/egusphere-2025-414
Preprint. Discussion started: 14 February 2025

introducing the minimal number of hydrological assumptions, hence a linear regression that also has the advantage to be conceptually extremely simple.

1.3 The synchronicity between precipitation and potential evaporation impacts annual streamflow totals

The fact that the synchronicity (i.e. the time shift) between precipitation and potential evaporation has a hydrological impact is known for a long time, as shown by a few precursors on this topic:

- Pardé published in 1933b a classic paper dedicated to the average flow of rivers, where he underlines that "for identical values of precipitation and temperature, everything else being equal, the runoff coefficient Q/P will be smaller where the larger part of precipitation falls during the warm season";
- Coutagne and de Martonne (1935) discussed formulas for annual streamflow, and underlined that formulas based only on the humidity ratio P/E_0 are deficient, because they fail to account for "the distribution of precipitations between seasons, in particular, in the temperate zone, between the warm and the cold season. Of two years of equal precipitation, the year which will receive the most part in summer will produce the less annual flow";
- Thornthwaite (1948) proposed to classify climates initially with two indices (one characterising the periods of water surplus and the other the periods of water deficiency), which he subsequently combined into a single index;
- Turc introduced in 1954 his famous formula for long-term actual evaporation. At the very end of his paper, he wrote that "the most urgent improvement" to his actual evaporation formula should be the introduction of the "distribution of precipitations and of the temperature changes within the year."

Recent studies also discussed the impact of climate seasonality on water balance, based on either theoretical or empirical approaches:

- among the theoretical studies, one can cite Dooge (1992) who presented catchment yield curves where he introduced as a parameter the length of the dry season; Milly (1994) who proposed a theoretical computation of actual evaporation based on the seasonality of the aridity index; Yokoo et al. (2008) who made theoretical computations on the difference between in-phase and out-of-phase regimes of precipitation and potential evapotranspiration; as well

https://doi.org/10.5194/egusphere-2025-414
Preprint. Discussion started: 14 February 2025

as Roderick and Farquhar (2011), Feng et al. (2012) and Donohue et al. (2012) who all made notable developments;

- The empirical study of Potter et al. (2005) quantified the impact of rainfall seasonality on mean annual water balance in Australia. Hickel and Zhang (2006) discussed the antagonistic effects of climate seasonality and soil moisture storage. de Lavenne and Andréassian (2018) proposed a synchronicity index to characterise the phase difference between precipitation and potential evaporation. Finally, Feng et al. (2019) proposed an index of asynchronicity for Mediterranean climates.

1.4 Purpose of the paper

In this paper, we wish to demonstrate exclusively through data analysis that anomalies in the seasonality of rainfall represent the second most important factor explaining annual streamflow anomalies (after precipitation but before potential evaporation). We also wish to show how introducing the synchronicity between precipitation and potential evaporation as an independent variable improves the prediction of annual streamflow variability.

2 Test catchments

2.1 Origin of the dataset

As presented in Table 1, we use catchments from nine countries to base our analysis on a wide range of climates.

https://doi.org/10.5194/egusphere-2025-414
Preprint. Discussion started: 14 February 2025

Table 1. Origin of the catchments used in this paper

Country	Number of catchments selected	Number of catchments available in the original dataset	Dataset	Reference
Australia	546	561	Camels-AUS	Fowler et al. (2024)
Brazil	636	734	Cabra	Almagro et al. (2021)
Denmark	202	304	Camels-DK	Liu et al. (2024)
France	628	654	Camels-FR	Delaigue et al. (2024)
Germany	1094	1555	Camels-DE	Loritz et al. (2024)
Sweden	152	158	Selection by G. Lindström	de Lavenne et al. (2022)
Switzerland	73	331	Camels-CH	Höge et al. (2023)
United Kingdom	136	670	Camels-UK	Coxon et al. (2020)
USA	655	672	Camels-US	Addor et al. (2017)

The total number of catchments is 4122, for a total of 162,005 station-years (the average length of catchment time series is 39 years). We use hydrological years as defined in the Notations section.

2.2 Catchment selection

The catchments used in this paper are selected from several datasets indicated in Table 1 and represent approximately 75% of the original catchments. Our catchment selection is based on:

1. **record length:** selected catchments have all more than 20 annual values;
2. **catchment memory:** selected catchments exhibit no or little interannual memory (as per de Lavenne et al., 2022) because the equation used to estimate streamflow elasticity is only hydrologically warranted for those catchments displaying no or little interannual memory (we wished to warrant a straightforward computation of the annual elasticity coefficients, based on annual average values only);
3. **regulations:** we removed the catchments that the authors of the datasets identified as significantly regulated by reservoirs (we either asked the datasets authors, or, where the information was available, set a limit equal to 10 mm equivalent volume storage in dams). For Switzerland, we considered the list of almost natural catchments published by Muelchi et al. (2022).

https://doi.org/10.5194/egusphere-2025-414
Preprint. Discussion started: 14 February 2025

2.3 Climatic inputs

Where several precipitation products were available in the original dataset, we used the product recommended by dataset authors as being of best quality, avoiding precipitation data based exclusively on satellite estimates.

Because potential evaporation was computed with different formulas in the different datasets, we recomputed it for all catchments using the formula proposed by Oudin et al. (2005), which requires extraterrestrial radiation and air temperature only. On one hand, this formula could be computed given the available data for all datasets, on the other hand it has been widely used worldwide and appears to be appropriate (while of course not perfect) to describe the atmospheric evaporative demand.

2.4 Characteristics of the catchment set

In our dataset, the aridity indices range from 0.1 to 6.3, with a first quartile equal to 0.6 and a third quartile equal to 1.0. The mean and the median of the aridity index equal both 0.8. In order to assess the generality of the results, we will discuss them at the country scale and also by climatic classes following the Köppen-Geiger classification (see e.g. Peel et al. 2007 and Table 2). Note that because we did not consider climatic zones with less than 100 catchments, the 384 catchments belonging to the less represented zones are left out of the Koppen-Geiger based analysis.

Table 2. Main climatic zones (in the sense of the Köppen-Geiger classification) represented in our dataset (we only present the zones counting more than 100 catchments)

Köppen-Geiger zone	Name	Number of catchments
Aw	Tropical savanna climate with dry winter	344
Cfa	Temperate climate without dry season with hot summer	364
Cfb	Temperate climate without dry season with warm summer	1746
Csa	Temperate climate with dry and hot summers	196
Dfb	Continental climate without dry season with warm summer	956
Dfc	Continental climate without dry season with cold summer	132

Last, we present in Figure 1 the 4122 catchments of our dataset in two variants of the Turc-Budyko non-dimensional graph. On the left-hand graph, each catchment corresponds to one point, whose coordinates correspond to the average aridity on the

https://doi.org/10.5194/egusphere-2025-414
Preprint. Discussion started: 14 February 2025

x-axis and 'actual evaporation' yield ((P-Q)/P) on the y-axis. On the right-hand graph, each catchment corresponds to one point, whose coordinates correspond to the average humidity on the x-axis and average streamflow yield (Q/P) on the y-axis.

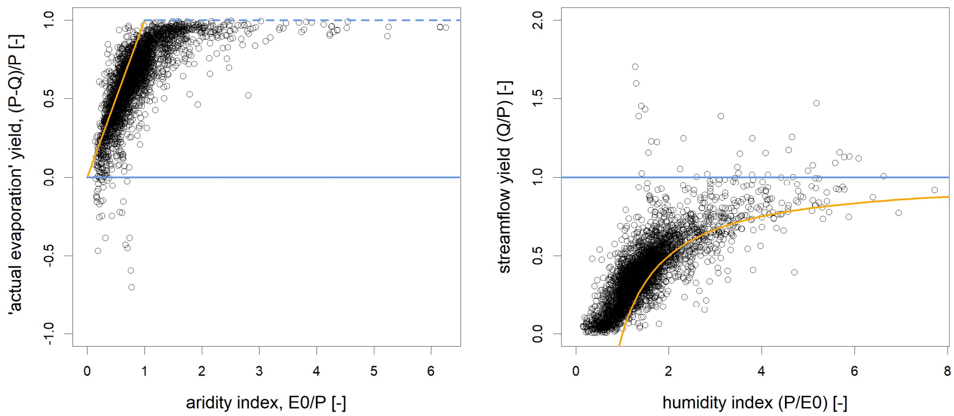

Figure 1: representation of the 4122 catchments in two equivalent forms of the Turc-Budyko non-dimensional space. The solid blue line corresponds to the water limit (Q=P) and the orange line corresponds to the energy limit (Q=P-E_0). On the left, an additional limit (dotted blue line) is sometimes improperly referred as "water limit" in the literature, but it only corresponds to the physical limit (Q=0), when one estimates the actual evaporation as the difference between discharge and precipitation. The catchments that are beyond the orange line (i.e. above on the left and below on the right) are "leaky" (in the sense that they contribute to the recharge of a regional aquifer) and those which are beyond the blue line (i.e. below on the left and above on the right) are "gaining" in the sense of a karstic catchment which would drain a larger than specified catchment.

3 Method

3.1 Computation of the synchronicity of precipitation and potential evaporation

In this paper, synchronicity between precipitation P and potential evapotranspiration E_0 is measured for each hydrological year n as follows:

We first compute the synchronous precipitation index λ_n, as in de Lavenne and Andréassian (2018):

https://doi.org/10.5194/egusphere-2025-414
Preprint. Discussion started: 14 February 2025

$$\lambda_n = \frac{\sum_{m=1}^{12}\left(P_{m,n} \cap E_{0_{m,n}}\right)}{\sum_{m=1}^{12}\left(P_{m,n} \cup E_{0_{m,n}}\right)} \quad \textbf{Eq. 1}$$

where the index *m* refers to the calendar month.

Because λ_n is nondimensional, we then rescale λ_n using the long-term average of the denominator of Eq. 1:

$$\Lambda_n = \lambda_n * \overline{\sum_{m=1}^{12}\left(P_{m,n} \cup E_{0_{m,n}}\right)} \quad \textbf{Eq. 2}$$

Note that:

- while Λ_n is an annual value, its computation requires the knowledge of the climate forcing at the monthly time step;
- dividing $\sum_{m=1}^{12}\left(P_{m,n} \cap E_{0_{m,n}}\right)$ by $\sum_{m=1}^{12}\left(P_{m,n} \cup E_{0_{m,n}}\right)$ is a necessity for regression analysis, because we cannot (or at least should not) introduce in a regression independent explanatory variables which are significantly correlated;
- λ_n represents the percentage of annual precipitation that is the most easily accessible to evaporation, and Λ_n (in mm/y) can be interpreted as representing the corresponding annual precipitation amount: for two years with the same annual amounts of precipitation and potential evaporation, Λ will reach higher values when P and E_0 are synchronous, and lower values when they are out of phase.

3.2 Computation of streamflow elasticities

To compute the streamflow elasticities, we will solve here the two following linear equations:

$$\Delta Q_n = e_{Q/P}\Delta P_n + e_{Q/E_0}\Delta E_{0_n} \quad \textbf{Eq. 3}$$

$$\Delta Q_n = e_{Q/E_0}\Delta P_n + e_{Q/E_0}\Delta E_{0_n} + e_{Q/\Lambda}\Delta\Lambda_n \quad \textbf{Eq. 4}$$

where ΔV_n is the deviation from the mean annual value (anomaly) for variable V (in mm/y) and $e_{Q/V}$ is the elasticity of streamflow against V (dimensionless).

Eq. 3 represents the classical approach to elasticity computation (see e.g. Andréassian et al., 2016). Eq. 4 represents the original contribution of this paper, and aims at determining how far climatic synchronicity explains annual streamflow variability.

Note that:

https://doi.org/10.5194/egusphere-2025-414
Preprint. Discussion started: 14 February 2025

- the estimation of elasticities in Eq. 3 and Eq. 4 are obtained via ordinary least squares (OLS). More complex statistical models such as generalised least squares are not required because the selected catchments do not exhibit a memory longer than a year, as explained in the data section (this guarantees the absence of streamflow autocorrelation which is a key statistical assumption behind OLS);
- when presenting the results, one has to decide of an appropriate statistical significance *p*-value threshold (which is of course a matter of convention). For this paper, we chose a threshold of 0.05;
- we compute elasticity coefficients between anomalies of equal dimensions (in mm/y), and not between relative anomalies (in %) because it allows a direct physical interpretation of the values of the coefficients;
- Eq. 3 and Eq. 4 were solved on a catchment-by-catchment basis, i.e. we computed 4122 distinct regressions.

4 Results

4.1 Graphical analysis of anomalies by country

To give a general picture of the correlation between streamflow anomalies and climatic anomalies, Figure 2 presents an aggregated plot for each of the country datasets, where we combine the anomalies of all catchments. At this scale, only general trends are apparent:

- as expected, streamflow anomaly is clearly positively correlated with precipitation anomaly in all countries;
- streamflow anomaly is overall very weakly negatively correlated with potential evaporation anomaly, Denmark being the only outlier where a weak positive correlation is identified (it is mainly due to the year 1990, which was in Denmark very dry year but with an unusual cold summer);
- streamflow anomaly is clearly negatively correlated to the synchronicity index anomaly Λ for all countries. The negative correlation means that years with a lower Λ (i.e. when precipitation and potential evaporation are more out of phase) yield more streamflow: this seems perfectly hydro-logical, and conforms to the general observations already identified by Pardé (1933a);

https://doi.org/10.5194/egusphere-2025-414
Preprint. Discussion started: 14 February 2025

- overall, the only surprising fact is that streamflow anomaly appears clearly more correlated to the synchronicity index anomaly than to the potential evaporation anomaly.

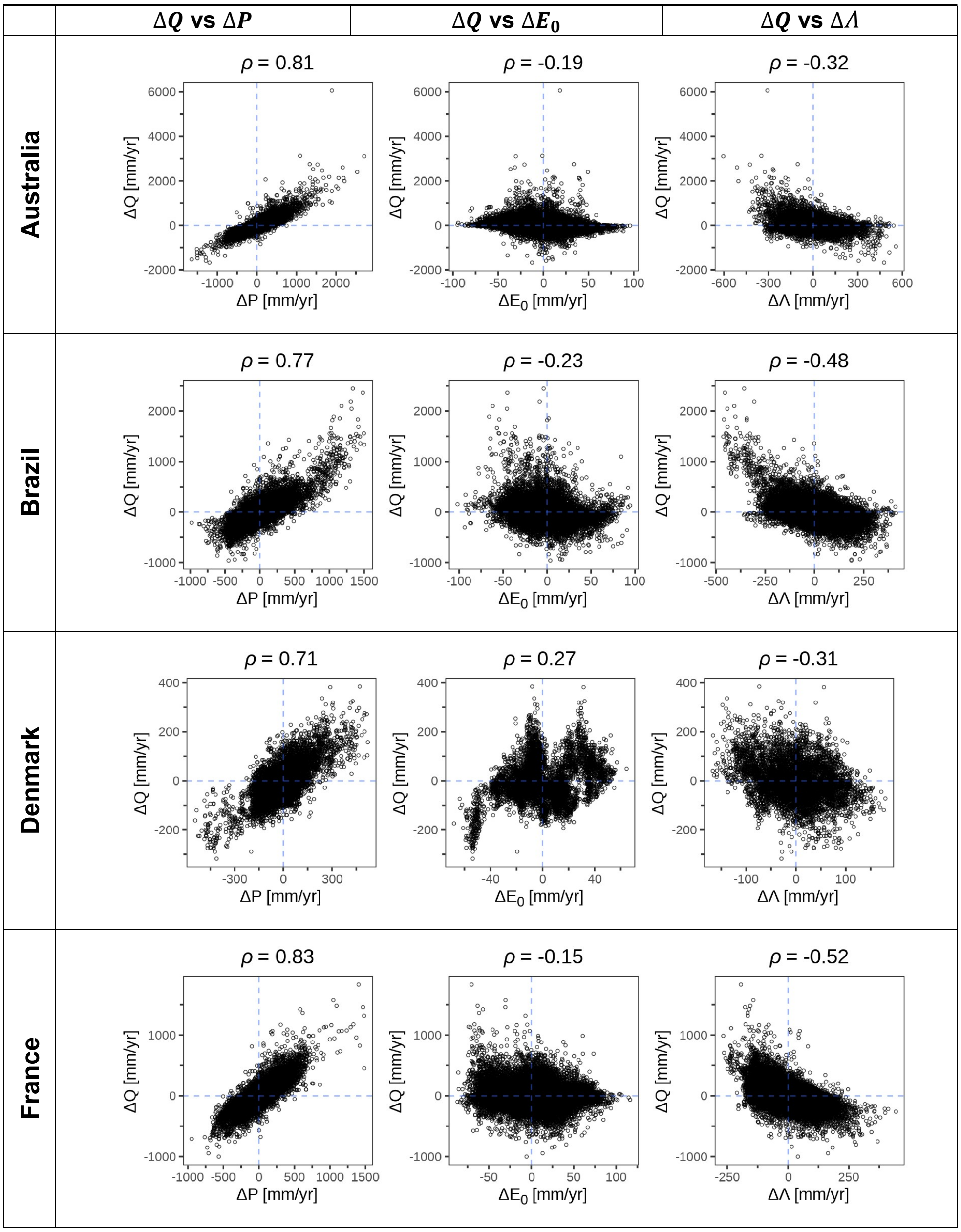

https://doi.org/10.5194/egusphere-2025-414
Preprint. Discussion started: 14 February 2025

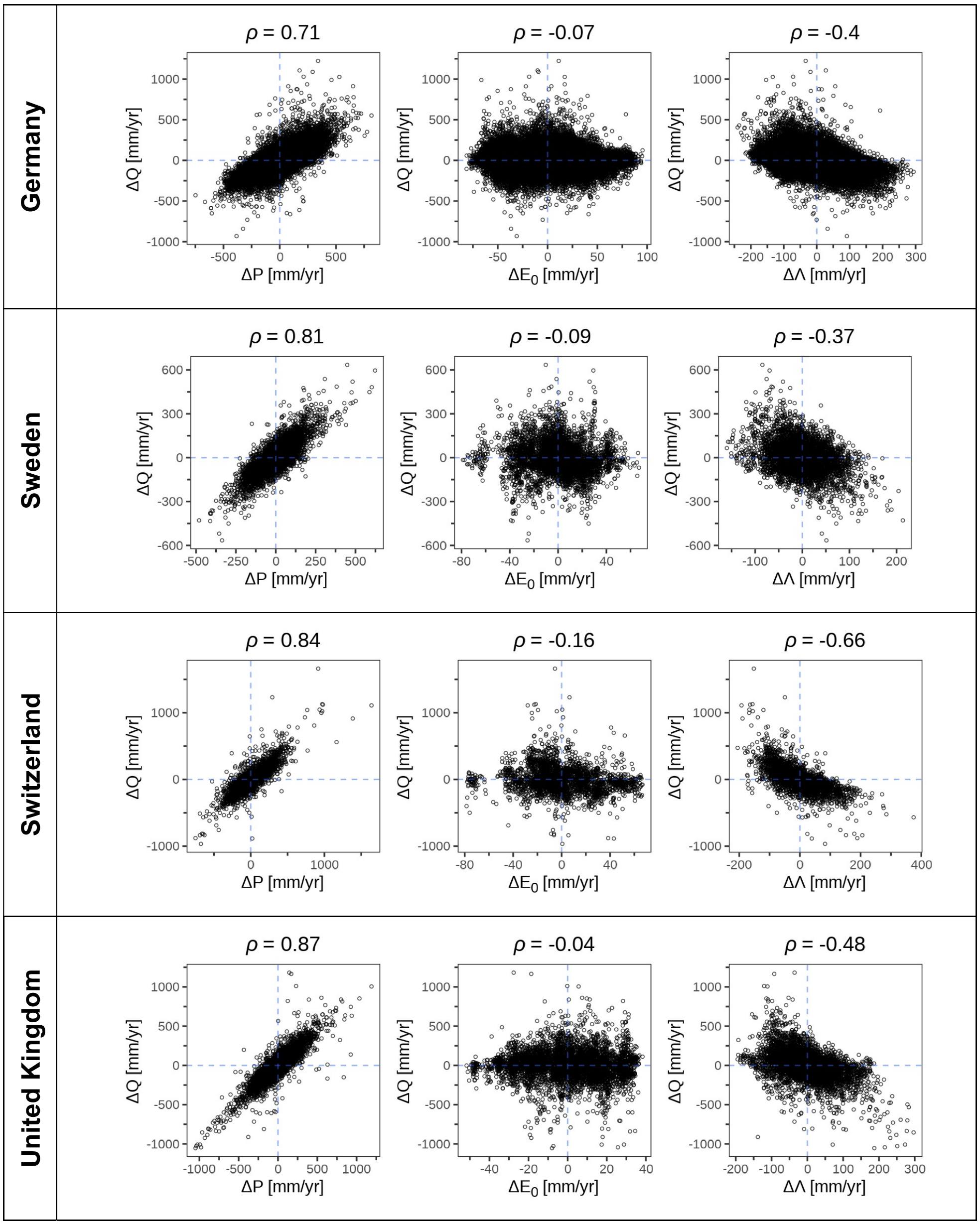

241

https://doi.org/10.5194/egusphere-2025-414
Preprint. Discussion started: 14 February 2025

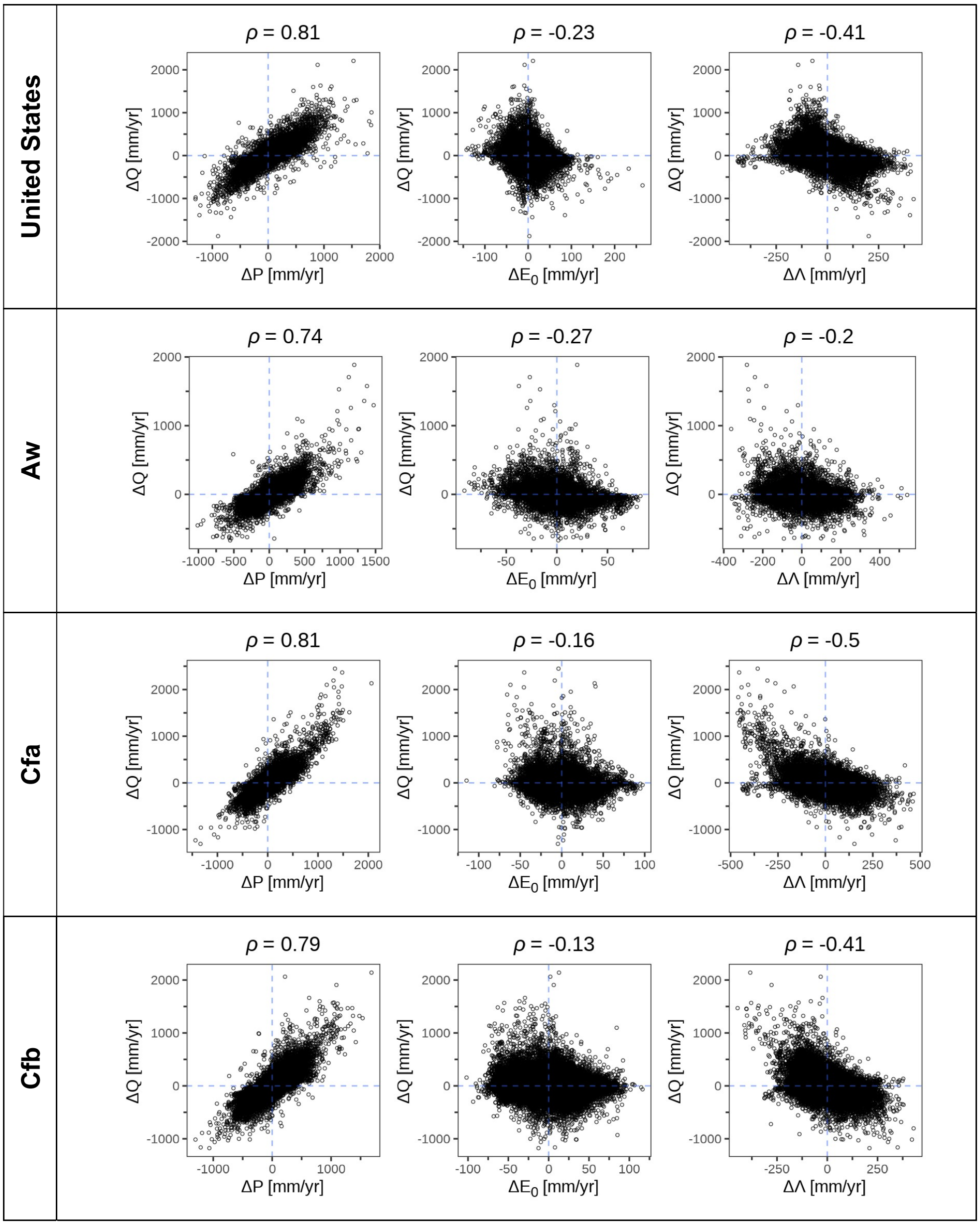

242

https://doi.org/10.5194/egusphere-2025-414
Preprint. Discussion started: 14 February 2025

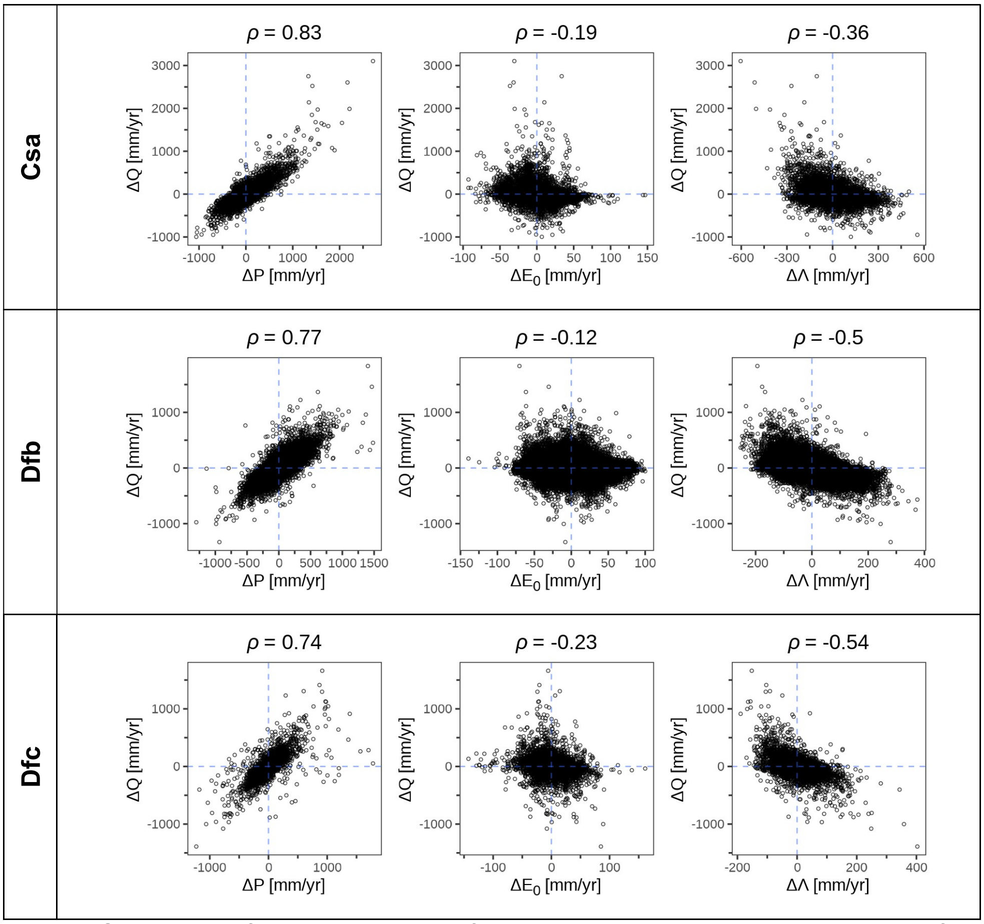

Figure 2. Scatter plots, for each country and for the main climate classes, between streamflow anomalies ΔQ, and: precipitation anomalies ΔP (left), potential evaporation anomalies ΔE_0 (middle) and synchronicity index anomalies $\Delta\Lambda$ (right). Each point represents one station-year. Above the graph, we have computed the corresponding Pearson correlation

4.2 An example at catchment scale: the Meurthe River @ Raon-l'Étape

We now show one example chosen in France, the Meurthe River (727 km²): on this catchment, with Köppen climate Cfb, annual streamflow anomalies show (Figure 3) a well-defined dependency to both precipitation and synchronicity anomalies, the dependency to potential evaporation anomaly being very weak.

https://doi.org/10.5194/egusphere-2025-414
Preprint. Discussion started: 14 February 2025

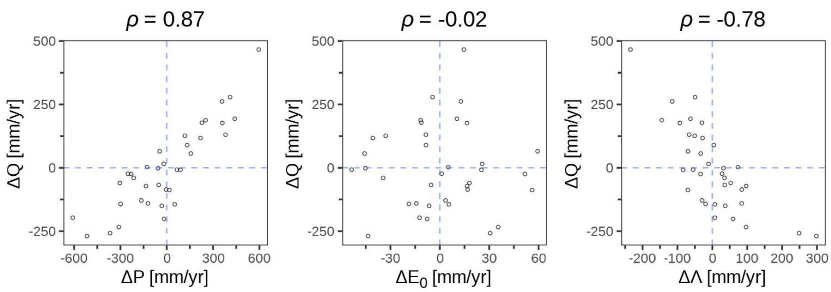

Figure 3. Example of an elasticity plot for the Meurthe River @ Raon-l'Étape (A615103001): each point corresponds to one hydrological year (for this catchment, 36 hydrological years were available, from 1975 to 2021). The Pearson correlations of ΔQ with ΔP, ΔE_0 and $\Delta \Lambda$ are respectively 0.87, -0.02 and -0.78

The visual impression is confirmed by the results of the linear regressions of Eq. 3 and Eq. 4 (Table 3), with values of the Student t-test indicating that precipitation has a very significant contribution, while the contribution of potential evaporation is not significant. The introduction of the synchronicity increases the R^2 (from 0.75 to 0.80) but the potential evaporation elasticity estimate remains not significant.

Table 3. Climate elasticity coefficients computed with and without the inclusion of the synchronicity variable Λ for the example catchment (La Meurthe @ Raon-l'Étape)

Formulation	$e_{Q/P}$[-]	p-value for $e_{Q/P}$	e_{Q/E_0}[-]	p-value for e_{Q/E_0}	$e_{Q/\Lambda}$[-]	p-value for $e_{Q/\Lambda}$	R^2
$\Delta Q = f(\Delta P, \Delta E_0)$	0.52	*< 0.001*	0.00	*0.99*	–	–	0.75
$\Delta Q = f(\Delta P, \Delta E_0, \Delta \Lambda)$	0.38	*< 0.001*	-0.25	*0.59*	-0.56	*< 0.01*	0.80

4.3 Overall results

We now analyse the results obtained for the 4122 catchments. Table 4 shows the statistics of the individual regressions, when no synchronicity is used (the classical case). It shows that for all the countries and all the climate groups:

- the value of the precipitation elasticity of streamflow is almost always significant at the 0.05 level;
- the value of the potential evaporation elasticity of streamflow is not frequently significant at the 0.05 level;

https://doi.org/10.5194/egusphere-2025-414
Preprint. Discussion started: 14 February 2025

- regression allows identifying values of precipitation elasticity which are almost always (i.e. for 93% of the catchments worldwide, and at the minimum for 80% of the cases for the different groupings) physically-realistic, i.e. comprised between 0 and 1.

Table 4. Linear regression results by country for Eq. 3 when regression uses two independent variables *P* and E_0 to explain streamflow anomaly

Region or climate class	Total number of catchments	Percentage of catchments where $e_{Q/P}$ was		Percentage of catchments where e_{Q/E_0} was		Mean R^2
		significant at the 0.05 level	*significant and in the range [0,1]*	significant at the 0.05 level	*significant and* in the range [-1,0]	
By country						
Australia	546	100%	97%	18%	9%	0.68
Brazil	636	95%	86%	12%	4%	0.64
Denmark	202	100%	100%	9%	0%	0.55
France	628	100%	93%	21%	7%	0.73
Germany	1094	94%	93%	18%	9%	0.50
Sweden	152	100%	87%	20%	7%	0.68
Switzerl.	73	100%	86%	8%	0%	0.77
UK	136	99%	89%	25%	2%	0.76
USA	655	99%	95%	9%	4%	0.67
By climate class						
Aw	344	93%	91%	16%	7%	0.62
Cfa	364	100%	90%	3%	0%	0.69
Cfb	1746	98%	94%	18%	7%	0.63
Csa	196	99%	96%	7%	1%	0.69
Dfb	956	96%	94%	21%	9%	0.58
Dfc	132	99%	80%	29%	10%	0.73
World	**4122**	**97%**	**93%**	**16%**	**6%**	**0.63**

Aw - Tropical savanna climate with dry winter, Cfa – Temperate climate without dry season with hot summer, Cfb – Temperate climate without dry season with warm summer, Csa – Temperate climate with dry and hot summers, Dfb – Continental climate without dry season with warm summer, Dfc – Continental climate without dry season with cold summer

Table 5 shows the same statistics, when the anomaly of synchronicity $\Delta\Lambda_n$ is introduced in the elasticity equation. It shows that:

- the average efficiency of the regression equation rises visibly for all the countries and all the climate groups (see also Figure 4). Naturally, an increase is expected when one adds an independent variable in a regression, but depending on the groups, the average additional explained variance varies between 3 % and 10 % (7 % globally), which we consider as significant;

https://doi.org/10.5194/egusphere-2025-414
Preprint. Discussion started: 14 February 2025

- for 64 % of the catchments, the anomaly of synchronicity $\Delta\Lambda_n$ is a significant contribution to the regression (to be compared to only 23 % for potential evaporation);
- introducing the anomaly of synchronicity $\Delta\Lambda_n$ does not modify the significance of the two other elasticity coefficients $e_{Q/P}$ and e_{Q/E_0}: we even have a slight increase of the proportion of catchments where e_{Q/E_0} coefficient is significant at the 0.05 level (from 16 % to 23 %);
- introducing the anomaly of synchronicity $\Delta\Lambda_n$ does not degrade the physical realism of the elasticity coefficients $e_{Q/P}$ and e_{Q/E_0}: we even have a slight increase of the proportion of catchments where $e_{Q/P}$ coefficient is significant and in the physical range [0,1] (from 93 % to 94 %) and where e_{Q/E_0} coefficient is significant and in the physical range [-1,0] (from 6 % to 11 %);
- there are only two countries (Switzerland and Brazil) and one climate type (*Dfc* – Continental climate without dry season with cold summer) which differ from the others by the lower relevance of the synchronicity index. Our interpretation of this lesser relevance is as follows: for Switzerland and climate zone Dfc we attribute it to the essentially energy-limited nature of the catchments (because we wanted catchments with minimal anthropogenic impact, we have selected in Switzerland essentially catchments at high elevations). Note however that in all groupings except Dfc, there are more catchments where $e_{Q/\Lambda}$ is significant at the 0.05 level than catchments where e_{Q/E_0} coefficient is significant at the same level.

https://doi.org/10.5194/egusphere-2025-414
Preprint. Discussion started: 14 February 2025

Table 5. Linear regression results by country for Eq. 4 when regression uses three independent variables to explain streamflow anomaly (to allow for comparison, the last column reports the mean R² of Table 4)

Country	Total number of catchments	Percentage of catchments where $e_{Q/P}$ was		Percentage of catchments where e_{Q/E_0} was		Percentage of catchments where $e_{Q/\Lambda}$ was		Mean R^2	*Mean R^2 from Table 4*
		significant at the 0.05 level	*significant and in the range [0,1]*	significant at the 0.05 level	*significant and in the range [-1,0]*	significant at the 0.05 level	*significant and in the range [-1,0]*		
By country									
Australia	546	100%	97%	41%	24%	87%	87%	0.78	*0.68*
Brazil	636	90%	83%	13%	5%	26%	25%	0.68	*0.64*
Denmark	202	98%	98%	7%	0%	43%	43%	0.60	*0.55*
France	628	99%	97%	27%	12%	82%	80%	0.79	*0.73*
Germany	1094	97%	96%	26%	16%	79%	78%	0.60	*0.50*
Sweden	152	100%	91%	23%	5%	40%	40%	0.72	*0.68*
Switzerl.	73	90%	75%	5%	0%	21%	19%	0.78	*0.77*
UK	136	99%	90%	38%	11%	62%	58%	0.82	*0.76*
USA	655	98%	96%	11%	4%	57%	52%	0.73	*0.68*
By climate class									
Aw	359	91%	90%	19%	11%	44%	44%	0.68	*0.62*
Cfa	364	97%	90%	9%	2%	52%	50%	0.75	*0.69*
Cfb	1746	99%	96%	27%	15%	76%	75%	0.71	*0.62*
Csa	197	98%	96%	19%	4%	46%	46%	0.74	*0.69*
Dfb	956	97%	96%	25%	13%	68%	65%	0.66	*0.58*
Dfc	132	96%	81%	28%	6%	27%	26%	0.76	*0.73*
World	**4122**	**97%**	**94%**	**23%**	**11%**	**64%**	**62%**	**0.70**	***0.63***

Aw - Tropical savanna climate with dry winter, Cfa – Temperate climate without dry season with hot summer, Cfb – Temperate climate without dry season with warm summer, Csa – Temperate climate with dry and hot summers, Dfb – Continental climate without dry season with warm summer, Dfc – Continental climate without dry season with cold summer

5 Discussion

Figure 4 illustrates the improvement of explanatory capacity in the regressions due to the introduction of the synchronicity anomalies. There is of course a lot of variability, as well as catchments for which the two regression models are equivalent (points on the 1:1 line) but overall the graph confirms visually that for many catchments (cf. the two third of the dataset where $e_{Q/\Lambda}$ was significant at the 0.05 level), accounting for synchronicity anomalies brings a visible improvement in the efficiency of the linear regression.

https://doi.org/10.5194/egusphere-2025-414
Preprint. Discussion started: 14 February 2025

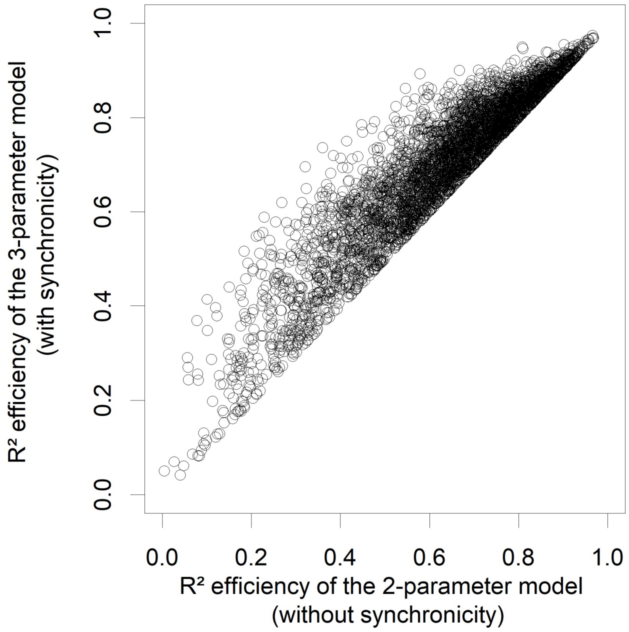

Figure 4. Comparison of the performances of the 2-parameter streamflow elasticity model (Eq. 3, which does not account for *P-E₀* synchronicity) and the 3-parameter model (Eq. 4, which does). Each point represents one of the 4122 catchments of our dataset

Also, Figure 5 shows the geographic distribution of the catchments where the P-E0 synchronicity had a significant contribution to explain streamflow anomalies (with a p-value threshold of 0.05). The map bring some further elements to Table 5 and illustrate that there are sub-regions where the coefficient $e_{Q/\Lambda}$ is mostly not significant at the 0.05 level. Based on our knowledge of the climatic specificities of each country, this seems to be possibly correlated to higher rainfall (cf. the Danish dataset, with the particular behavior of the West of Jutland, the case of Florida in the US, the case of the Scottish catchments in Great Britain) and/or to colder areas (cf. the Swiss, Swedish and US datasets).

https://doi.org/10.5194/egusphere-2025-414
Preprint. Discussion started: 14 February 2025

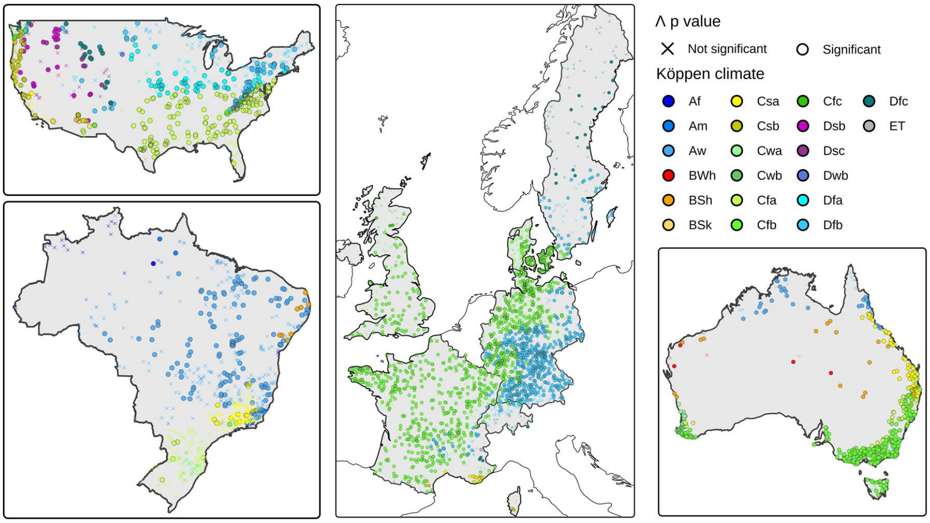

Figure 5. map of the 4122 catchments used in this study, each catchment is represented by either a circle (where the P-E_0 synchronicity anomalies had a significant contribution to explain streamflow anomalies) or a cross (where it was not significant at the 0.05 level). The color of circles and crosses corresponds to the Köppen climate classes

To verify this hypothesis, we have plotted in Figure 6 the p-values of the 4122 $e_{Q/\Lambda}$ coefficients as a function of the humidity index P/E_0: this graph clearly indicates that most of the humid catchments (Humidity index > 2) lack sensitivity to the P-E_0 seasonality, and this pattern is probably the main explication of the geographical patterns visible in Figure 5.

https://doi.org/10.5194/egusphere-2025-414
Preprint. Discussion started: 14 February 2025

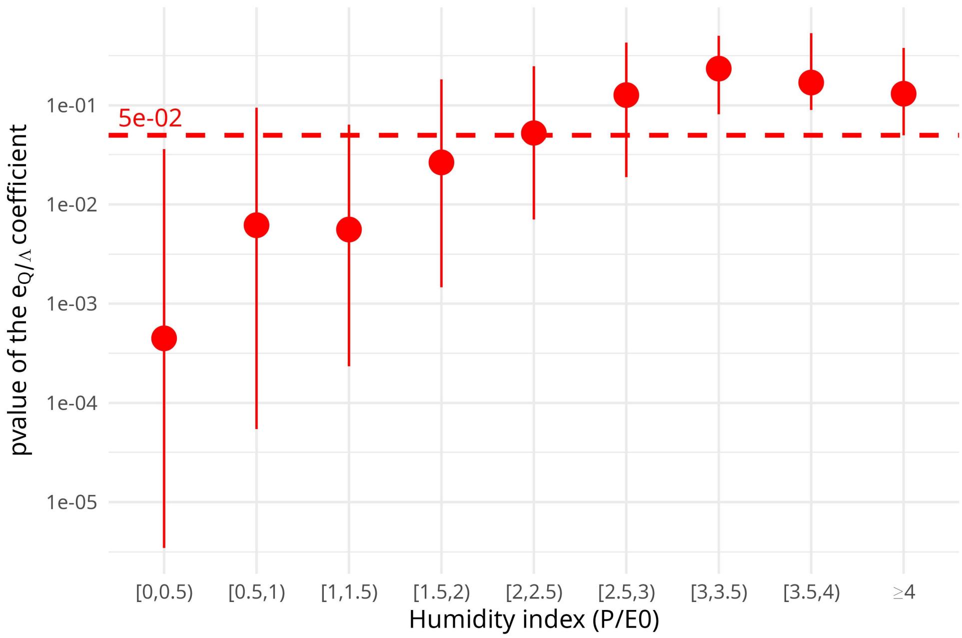

Figure 6: distribution of the p-values of the 4122 $e_{Q/\Lambda}$ coefficients as a function of the humidity index P/E0. The red points represent the median, the bar represent the interquartile range, and the dashed line represents the 0.05 threshold.

6 Conclusion

6.1 Synthesis

In this paper, we investigated the dependency between streamflow elasticity and the synchronicity of precipitation and potential evaporation, using a dataset of 4122 catchments located in Europe, Australia, North America and South America.

- we verified empirically the good correlation existing between streamflow anomalies, the anomalies of annual precipitation, and the anomalies of synchronous P-E_0 amounts;
- we demonstrated that the role of the synchronicity between P and E_0 is far more important to explain streamflow anomalies than the role of the anomalies of E_0;
- we showed that introducing the synchronicity between precipitation and potential evaporation as an independent variable in the linear regression clearly improves the prediction of annual streamflow variability.

https://doi.org/10.5194/egusphere-2025-414
Preprint. Discussion started: 14 February 2025

6.2 Perspectives

Notwithstanding with the above positive results, some estimated elasticity values remain outside of their physically acceptable domain (i.e. [0,1] for $e_{Q/P}$ and [-1,0] for e_{Q/E_0} and $e_{Q/\Lambda}$). For precipitation elasticity $e_{Q/P}$, we had 94% of the catchments in the physical range for a total of 97% of the catchments where precipitation elasticity was significant. For potential evaporation elasticity e_{Q/E_0}, lack of physical realism occurs in most of the cases (i.e. we had only 11% of the catchments in the physical range for a total of 23% of the catchments where potential evaporation elasticity was significant), very likely a problem of sensitivity in the regression, which causes this difficulty in obtaining realistic elasticity coefficients. Last for synchronicity elasticity $e_{Q/\Lambda}$, we had 62% of the catchments in the physical range for a total of 64% of the catchments where synchronicity elasticity was significant. In the future, we wish to investigate more alternative statistical models that could better constrain the identification of the elasticity coefficients within their physically realistic domain.

7 Acknowledgements

The authors would like to acknowledge the many individuals that worked to make available the hydrological datasets used in this paper. Special thanks are due to Charles Perrin and Guillaume Thirel for their reviews and suggestions and to Laurent Strohmenger for his help with the Köppen-Geiger classification.

8 Funding

This research has been funded in part by the Agence Nationale de la Recherche (projects CIPRHES ANR-20-CE04-0009 and DRHYM ANR-22-CE56-0007).

9 Author contributions

VA: conceptualization and writing, GMG: computations, figures, discussion, AL: computations, discussion, JL: discussion, writing (review and editing)

10 Competing interests

The authors declare that they have no conflict of interest.

https://doi.org/10.5194/egusphere-2025-414
Preprint. Discussion started: 14 February 2025

11 References

Addor, N., A. J. Newman, N. Mizukami, and M. P. Clark. 2017. The CAMELS data set: catchment attributes and meteorology for large-sample studies. Hydrol. Earth Syst. Sci., 21: 5293-5313. https://dx.doi.org/10.5194/hess-21-5293-2017

Almagro, A., Oliveira, P.T.S., Alves Meira Neta, A., Roy, T., Troch, P. 2021. CABra: a novel large-sample dataset for Brazilian catchments. Hydrol. Earth Syst. Sci., 25: 3105–3135. https://doi.org/10.5194/hess-25-3105-2021

Andréassian, V., L. Coron, J. Lerat, and N. Le Moine. 2016. Climate elasticity of streamflow revisited – an elasticity index based on long-term hydrometeorological records. Hydrol. Earth Syst. Sci., 20: 4503–4524, https://dx.doi.org/10.5194/hess-20-4503-2016

Chiew, F.H.S. 2006. Estimation of rainfall elasticity of streamflow in Australia. Hydrological Sciences Journal, 51: 613–625. https://doi.org/10.1623/hysj.51.4.613

Coutagne, A. and E. de Martonne. 1934. De l'eau qui tombe à l'eau qui coule – évaporation et déficit d'écoulement. IAHS, vol 97-128.

Coxon, G., N. Addor, J. P. Bloomfield, J. Freer, M. Fry, J. Hannaford, N. J. K. Howden, R. Lane, M. Lewis, E. L. Robinson, T. Wagener, and R. Woods. 2020. CAMELS-GB: hydrometeorological time series and landscape attributes for 671 catchments in Great Britain. Earth Syst. Sci. Data, 12: 2459-83. https://dx.doi.org/10.5194/essd-12-2459-2020

de Lavenne, A., V. Andréassian, L. Crochemore, G. Lindström, & B. Arheimer. 2022. Quantifying pluriannual hydrological memory with Catchment Forgetting Curves. Hydrol. Earth Syst. Sci., 26: 2715–2732, https://doi.org/10.5194/hess-26-2715-2022

de Lavenne, A. & V. Andréassian. 2018. Impact of climate seasonality on catchment yield: a parameterization for commonly-used water balance formulas. J. Hydrol., 558: 266–274. https://dx.doi.org/10.1016/j.jhydrol.2018.01.009

Delaigue, O., Mendoza Guimarães, G., Brigode, P., Génot, B., Perrin, C., Soubeyroux, J.M., Janet, B. Addor, N. & Andréassian, V. 2024. CAMELS-FR dataset: A large-sample hydroclimatic dataset for France to explore hydrological diversity and support model benchmarking. Earth Syst. Sci. Data Discuss. [preprint]. https://doi.org/10.5194/essd-2024-415

https://doi.org/10.5194/egusphere-2025-414
Preprint. Discussion started: 14 February 2025

Donohue, R., Roderick, M.L., McVicar, T.R. 2012. Roots, storms and soil pores: incorporating key ecohydrological processes into Budyko's hydrological model. J. Hydrol., 436-437: 35-50. https://doi.org/10.1016/j.jhydrol.2012.02.033

Dooge, J.C.I., 1992. Sensitivity of runoff to climate change: A Hortonian approach. Bulletin of the American Meteorological Society, 73: 2013-2024. https://doi.org/10.1175/1520-0477(1992)073<2013:SORTCC>2.0.CO;2

Feng, X., Vico, G., Porporato, A., 2012. On the effects of seasonality on soil water balance and plant growth. Water Resour. Res., 48. https://doi.org/10.1029/2011WR011263

Feng, X. Thompson, S.E., Woods, R., & Porporato, I. 2019. Quantifying asynchronicity of precipitation and potential evapotranspiration in Mediterranean climates. Geophysical Research Letters. https://doi.org/10.1029/2019GL085653

Fowler, K. J. A., Zhang, Z., and Hou, X.: CAMELS-AUS v2: updated hydrometeorological timeseries and landscape attributes for an enlarged set of catchments in Australia, Earth Syst. Sci. Data Discuss. [preprint], https://doi.org/10.5194/essd-2024-263, in review, 2024.

Hickel, K., Zhang, L., 2006. Estimating the impact of rainfall seasonality on mean annual water balance using a top-down approach. J. Hydrol. 331: 409–424. https://doi.org/10.1016/j.jhydrol.2006.05.028

Höge, M., Kauzlaric, M., Siber, R., Schönenberger, U., Horton, P., Schwanbeck, J. and Floriancic, M. G. and Viviroli, D. and Wilhelm, S. and Sikorska-Senoner, A.E., Addor, N., Brunner, M., Pool, S., Zappa, M. and Fenicia, F., 2023. CAMELS-CH: hydro-meteorological time series and landscape attributes for 331 catchments in hydrologic Switzerland. Earth Syst. Sci. Data, 15: 5755-5784. https://doi.org/10.5194/essd-15-5755-2023

Koster, R.D., and M.J. Suarez. 1999. A simple framework for examining the interannual variability of land surface moisture fluxes. Journal of Climate, 12: 1911-1917. https://doi.org/10.1175/1520-0442(1999)012<1911:ASFFET>2.0.CO;2

Leopold, L.B. 1974. Water: A Primer. WH Freeman & Co, 172 p.

Loritz, R., Dolich, A., Acuña Espinoza, E., Ebeling, P., Guse, B., Götte, J., Hassler, S. K., Hauffe, C., Heidbüchel, I., Kiesel, J., Mälicke, M., Müller-Thomy, H., Stölzle, M., and Tarasova, L. 2024. CAMELS-DE: hydro-meteorological time series and attributes for 1555 catchments in Germany, Earth Syst. Sci. Data Discuss. [preprint], https://doi.org/10.5194/essd-2024-318

https://doi.org/10.5194/egusphere-2025-414
Preprint. Discussion started: 14 February 2025

Liu, J., Koch, J., Stisen, S., Troldborg, L., Højberg, A. L., Thodsen, H., Hansen, M. F. T., and Schneider, R. J. M. 2024. CAMELS-DK: Hydrometeorological Time Series and Landscape Attributes for 3330 Catchments in Denmark, Earth Syst. Sci. Data Discuss. [preprint], https://doi.org/10.5194/essd-2024-292

Milly, P.C.D. 1994. Climate, interseasonal storage of soil water, and the annual water balance. Advances in Water Resources, 17(1–2), 19–24. https://doi.org/10.1016/0309-1708(94)90020-5

Muelchi, R., Rössler, O., Schwanbeck, J., Weingartner, R., Martius, O. 2022. An ensemble of daily simulated runoff data (1981–2099) under climate change conditions for 93 catchments in Switzerland (Hydro-CH2018-Runoff ensemble). Geosci Data J., 9: 46–57. https://doi.org/10.1002/gdj3.117

Oudin, L., Hervieu, F., Michel, C., Perrin, C., Andréassian, V., Anctil, F. & Loumagne, C. 2005. Which potential evapotranspiration input for a rainfall-runoff model? Part 2 – Towards a simple and efficient PE model for rainfall-runoff modelling. Journal of Hydrology, 303: 290-306, https://dx.doi.org/10.1016/j.jhydrol.2004.08.026

Pardé, M., 1933a. Fleuves et rivières. Armand Collin, Paris. 224 p.

Pardé, M., 1933b. L'abondance des cours d'eau. Revue de Géographie Alpine 21 (3) : 497–542. https://www.persee.fr/doc/rga_0035-1121_1933_num_21_3_5370

Peel, M.C., Finlayson, B.L., McMahon, T.A. 2007. Updated world map of the Köppen–Geiger climate classification, Hydrol. Earth System Sci., 11(5):1633-1644. https://doi.org/10.5194/hess-11-1633-2007

Potter, N.J., Zhang, L., Milly, P.C.D., McMahon, T.A., Jakeman, A.J., 2005. Effects of rainfall seasonality and soil moisture capacity on mean annual water balance for Australian catchments. Water Resour. Res. 41 (6). https://doi.org/10.1029/2004wr003697

Roderick, M.L., Farquhar, G.D., 2011. A simple framework for relating variations in runoff to variations in climatic conditions and catchment properties. Water Resour. Res., 47. https://doi.org/10.1029/2010WR009826

Sankarasubramanian, A., Vogel, R.M., Limbrunner, J.F., 2001. Climate elasticity of streamflow in the United States. Water Resour. Res., 37(6): 1771-1781. https://doi.org/10.1029/2000wr900330

Schaake, J., Liu, C., 1989. Development and application of simple water balance models to understand the relationship between climate and water resources, New Directions for Surface Water Modeling. IAHS Red Book series n°181,

https://doi.org/10.5194/egusphere-2025-414
Preprint. Discussion started: 14 February 2025

Wallingford, pp. 343-352. https://iahs.info/uploads/dms/7849.343-352-181-Schaake-Jr.pdf

Thornthwaite, C.W., 1948. An approach toward a rational classification of climate. Geog. Rev. 38 (1), 55–94. https://doi.org/10.2307/210739

Turc, L. 1954. The water balance of soils: relationship between precipitations, evaporation and flow (In French: Le bilan d'eau des sols: relation entre les précipitations, l'évaporation et l'écoulement), Annales Agronomiques, Série A, 491-595.

Yokoo, Y., Sivapalan, M., Oki, T. 2008. Investigating the role of climate seasonality and landscape characteristics on mean annual and monthly water balances. J. Hydrol. 357 (255–269). https://doi.org/10.1016/j.jhydrol.2008.05.010

12 Appendix: further details to justify our choice for the synchronicity index

There is no unique solution for choosing a measure of synchronicity between Precipitation and Potential Evaporation. In a previous paper (de Lavenne & Andréassian, 2018) we had presented a non-dimensional index (Eq. 1) which had the desirable properties, and this index proved again to be adapted in this study. We did however try to replace it with simpler versions, and we would like to present these alternatives in order to save time and effort for those who would like to keep working on this topic.

The first simplification which was tested (called here $S1$) consisted in using directly the numerator of the λ index as follows:

$$S1_n = \sum_{m=1}^{12} \left(P_{m,n} \cap E_{0_{m,n}}\right) \quad \textbf{Eq. 5}$$

$S1$ was an interesting solution because it yielded directly a value in [mm/y], without the need for rescaling, and it clearly represented the precipitation volume that was the most easily accessible to evaporation. In the linear regression, it did give very high average R² (world average of 0.70, the same as for the solution retained). The reason why we did not consider this solution was that there was a correlation between $\Delta S1$ and ΔP for many catchments (average correlation of +0.58 over the 4122 catchments,

https://doi.org/10.5194/egusphere-2025-414
Preprint. Discussion started: 14 February 2025

reaching +0.74 over the Australian catchments), and introducing two correlated variables in a regression equation is clearly bad statistical practice.

To avoid this high correlation, we tested a simplified version of the λ index, which we redimensionalized using the average interannual precipitation as in Eq. 6 below

$$S2(n) = \frac{\sum_{m=1}^{12}\left(P_{m,n} \cap E_{0_{m,n}}\right)}{P_n} * \bar{P} \qquad \textbf{Eq. 6}$$

The problem we found with $S2$ was that it yielded a constant value (equal to $\bar{P}$) for many arid catchments, where for most of the years $\frac{\sum_{m=1}^{12}\left(P_{m,n} \cap E_{0_{m,n}}\right)}{P_n} = 1$ because $P_{m,n} \ll E_{0_{m,n}}$.

This is why we opted for using the original λ index (which never reaches 1, and which correlation with the annual P is low: -0.18 on average). Redimensionalizing λ was logically made by multiplying it by $\overline{\sum_{m=1}^{12}\left(P_{m,n} \cup E_{0_{m,n}}\right)}$, which is a constant value for each catchment and does not modify the correlation with P_n. This yielded Λ_n, which has the desired dimension (mm/y), and was used throughout this paper.

$$\Lambda_n = \frac{\sum_{m=1}^{12}\left(P_{m,n} \cap E_{0_{m,n}}\right)}{\sum_{m=1}^{12}\left(P_{m,n} \cup E_{0_{m,n}}\right)} * \overline{\sum_{m=1}^{12}\left(P_{m,n} \cup E_{0_{m,n}}\right)} \qquad \textbf{Eq.1}$$